Absence versus Presence of Dissipative Quantum Phase Transition in Josephson Junctions

Kanta Masuki,[1,*] Hiroyuki Sudo,[1] Masaki Oshikawa,[2,3] and Yuto Ashida[1,4,†]

[1]*Department of Physics, University of Tokyo, 7-3-1 Hongo, Bunkyo-ku, Tokyo 113-0033, Japan*
[2]*Institute for Solid State Physics, University of Tokyo, Kashiwa, Chiba 277-8581, Japan*
[3]*Kavli Institute for the Physics and Mathematics of the Universe (WPI), University of Tokyo, Kashiwa, Chiba 277-8583, Japan*
[4]*Institute for Physics of Intelligence, University of Tokyo, 7-3-1 Hongo, Tokyo 113-0033, Japan*

(Received 28 November 2021; revised 3 March 2022; accepted 27 July 2022; published 17 August 2022)

Dissipative quantum phase transition has been widely believed to occur in a Josephson junction coupled to a resistor despite a lack of concrete experimental evidence. Here, on the basis of both numerical and analytical nonperturbative renormalization group analyses, we reveal breakdown of previous perturbative arguments and defy the common wisdom that the transition always occurs at the quantum resistance $R_Q = h/(4e^2)$. We find that renormalization group flows in nonperturbative regimes induce nonmonotonic renormalization of the charging energy and lead to a qualitatively different phase diagram, where the insulator phase is strongly suppressed to the deep charge regime (Cooper pair box), while the system is always superconducting in the transmon regime. We identify a previously overlooked dangerously irrelevant term as an origin of the failure of conventional understandings. Our predictions can be tested in recent experiments realizing high-impedance long superconducting waveguides and would provide a solution to the long-standing controversy about the fate of dissipative quantum phase transition in the resistively shunted Josephson junction.

DOI: 10.1103/PhysRevLett.129.087001

Understanding physical properties of quantum systems interacting with environmental degrees of freedom is one of the central problems in quantum many-body physics. A wide variety of intriguing quantum phenomena have been revealed in the last half century; key examples include the Kondo problem in heavy fermion materials or mesoscopic structures [1–5], transport through quantum nanowire systems [6–10], and quantum dissipative systems [11–14]. One of the most notable predictions among such fundamental problems is the dissipative quantum phase transition (DQPT) occurring in the resistively shunted Josephson junction (RSJ) [15–21]. Previous studies [22–25] predicted that the Josephson junction (JJ) at zero temperature remains superconducting below the quantum resistance $R < R_Q = h/(4e^2)$ while it becomes insulator (or precisely normal metal) in $R > R_Q$. This result has been obtained by such theoretical methods as perturbative renormalization group (RG) analysis [22–29] and path-integral Monte Carlo method [30–32]. While experimental attempts to observe DQPT have been made [33–37], interpretation of these results has remained a matter of debate [30,36,38–40]. In particular, a possible absence of DQPT in the predicted parameter regime has been recently reported [38]. All in all, despite many years of research, a comprehensive understanding of DQPT has yet to be achieved.

The aim of this Letter is to fill this gap and provide a solution to the long-standing controversy regarding DQPT. To this end, we systematically analyze RSJ on the basis of numerical and analytical nonperturbative approaches, namely, numerical renormalization group (NRG) and functional renormalization group (FRG). Surprisingly, both analyses lead to the ground-state phase diagram (Fig. 1)

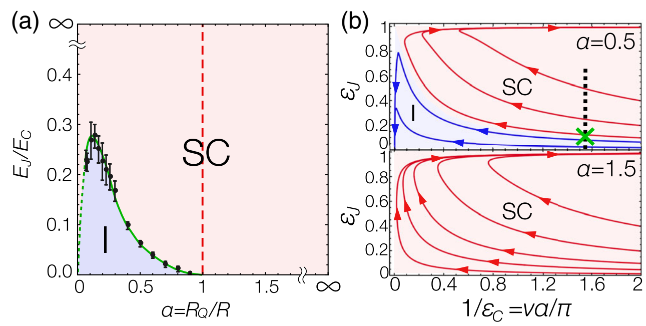

FIG. 1. (a) Ground-state phase diagram of RSJ. Green curve indicates the phase boundary determined from NRG, separating the superconducting (SC) and insulator (I) phases. Red vertical dashed line is the commonly believed boundary. (b) FRG flow diagrams of dimensionless Josephson (charging) energy $\epsilon_{J(C)}$ at different dissipation strengths α. At UV scale $\epsilon_{J,C} \ll 1$, Josephson coupling ϵ_J is always relevant and triggers nonmonotonic renormalization of dangerously irrelevant term $\nu \propto 1/\epsilon_C$. Transition occurs at finite E_J/E_C in $\alpha < 1$ (green cross in top panel), while the system always flows to the SC fixed point in $\alpha > 1$ (bottom panel). Previous perturbative results are reproduced in the limit $\nu \propto 1/\epsilon_C \to 0$.

that is dramatically different from the one expected from the previous arguments. Specifically, the insulator phase is strongly suppressed to the deep charge regime $E_J/E_C \ll 1$ (Cooper pair box) while the system is always superconducting in the transmon regime $E_J/E_C \gg 1$, where E_J is the Josephson coupling and $E_C = (2e)^2/2C_J$ is the charging energy with the capacitance C_J. In particular, as $\alpha = R_Q/R$ is decreased, our results indicate the reentrant transition from insulating to superconducting phase in $\alpha \ll 1$ (see also Fig. 4 below). These findings sharply contrast with the common wisdom that the transition should occur at $R = R_Q$ for any E_J/E_C [red dashed line in Fig. 1(a)].

While the conventional understanding at an early stage was made by perturbative analyses and duality argument, we point out that these previous considerations implicitly discarded a term (which we call the capacitance term $\nu \propto 1/E_C$) that was expected to be irrelevant from dimensional counting [24,41]. We show that this previously overlooked term is actually "dangerously irrelevant," i.e., it can turn into relevant at low-energy scales due to nonperturbative renormalization [Fig. 1(b)]. It is this subtle, yet crucial missing piece that completes our understanding of DQPT and explains the failure of the previous arguments.

From a broader perspective, small quantum systems interacting with a bosonic bath as studied here are fairly ubiquitous in, e.g., electron-phonon systems and quantum light-matter systems. Our analyses should have a broad range of applications to those systems, which are currently the subject of intense research in different fields. Moreover, in view of the fundamental role of JJ in quantum circuits [42–49], the present study will also advance our understanding of the interaction between quantum information processors and electromagnetic environments in general.

Model.—We consider the following RSJ Hamiltonian, in which JJ couples to the environmental degrees of freedom represented as a collection of harmonic oscillators [11]:

$$\hat{H} = E_C(\hat{N} - \hat{n}_r)^2 - E_J\cos(\varphi) + \sum_{0<k\le K} \hbar\omega_k \hat{a}_k^\dagger \hat{a}_k, \qquad (1)$$

$$\hat{n}_r = \frac{\sqrt{\alpha}}{2\pi} \sum_{0<k\le K} \sqrt{\frac{2\pi}{kL}}(\hat{a}_k^\dagger + \hat{a}_k), \qquad (2)$$

where φ is the JJ phase, $\hat{N} = -i\partial/\partial\varphi$ is the charge operator, bath frequencies are $\omega_k = vk = vm\pi/L$ with $m = 1, 2, \ldots M$, $K = M\pi/L$ is the wave number cutoff, and $\hat{a}_k$ ($\hat{a}_k^\dagger$) is the bosonic annihilation (creation) operator of mode k. The constants v and L have the dimensions of velocity and length, and $\alpha = R_Q/R$ is the dimensionless frictional coefficient. We remark that Eq. (1) takes the same form as in quantum light-matter Hamiltonian under the long-wavelength approximation [50]. Below we aim to extract its physical properties in the wideband condition $E_{J,C} \ll \hbar W$ and thermodynamic limit $L \to \infty$, where we denote the frequency cutoff as $W = vK$.

We first diagonalize the quadratic part, $E_C\hat{n}_r^2 + \sum_k \hbar\omega_k \hat{a}_k^\dagger \hat{a}_k$, via the Bogoliubov transformation and rewrite the Hamiltonian in Eq. (1) as (see, e.g., Ref. [41])

$$\hat{H} = E_C\hat{N}^2 - E_J\cos(\varphi) - \hat{N}\sum_{0<k\le K} \hbar g_k(\hat{b}_k + \hat{b}_k^\dagger) + \sum_{0<k\le K} \hbar\omega_k \hat{b}_k^\dagger \hat{b}_k, \qquad (3)$$

$$g_k = \sqrt{\frac{2\pi v}{\alpha L}\frac{\omega_k}{1 + (\frac{\nu\omega_k}{W})^2}}, \qquad \nu \equiv \frac{\pi}{\alpha\epsilon_C}, \qquad \epsilon_C = \frac{E_C}{\hbar W}, \qquad (4)$$

where we introduce the squeezed annihilation (creation) operators $\hat{b}_k$ ($\hat{b}_k^\dagger$). The Hamiltonian in Eq. (3) can also be derived from a microscopic model of JJ shunted by a transmission line with impedance R, length L, and propagation speed v [51]. A salient feature is that the capacitive coupling g_k acquires suppression at frequencies higher than $W/\nu = \alpha E_C/(\pi\hbar)$ [52–54]. This natural cutoff frequency, $\alpha E_C/(\pi\hbar)$, depends only on the model parameters and our results are independent of a choice of W as long as the wideband condition, $W \gg \alpha E_C/(\pi\hbar)$, is satisfied.

To perform the NRG analysis [55], we next use a unitary transformation $\hat{U} = \exp(-i\hat{N}\hat{\Xi})$ with $\hat{\Xi} = i\sum_k (g_k/\omega_k)\times(\hat{b}_k^\dagger - \hat{b}_k)$ [56]. Introducing the field operators $\hat{\phi}(x)$ and $\hat{\pi}(x)$,

$$\hat{\phi}(x) = \sqrt{\alpha}\varphi + \sum_{0<k\le K} \sqrt{\frac{2\pi}{kL}} i(\hat{b}_k - \hat{b}_k^\dagger)\cos(kx), \qquad (5)$$

$$\hat{\pi}(x) = \sum_{0<k\le K} \sqrt{\frac{2\pi k}{L}}(\hat{b}_k + \hat{b}_k^\dagger)\sin(kx), \qquad (6)$$

we obtain the transformed Hamiltonian $\hat{H}_U \equiv \hat{U}^\dagger \hat{H}\hat{U}$,

$$\hat{H}_U = -E_J\cos\left[\frac{1}{\sqrt{\alpha}}\int_0^L dx\hat{\phi}(x)f_\nu(x)\right] + \hat{H}_{\mathrm{TLL}}, \qquad (7)$$

where $\hat{H}_{\mathrm{TLL}}$ is the Tomonaga-Luttinger liquid Hamiltonian and $f_\nu(x)$ is the function that exponentially vanishes on the length scale $\nu/K = \pi\hbar v/(\alpha E_C)$ as follows:

$$\hat{H}_{\mathrm{TLL}} = \frac{\hbar v}{4\pi}\int_0^L dx\{[\partial_x\hat{\phi}(x)]^2 + \hat{\pi}(x)^2\}, \qquad (8)$$

$$f_\nu(x) = \frac{2}{\pi}\int_0^K dk \frac{\cos(kx)}{\sqrt{1 + (\nu k/K)^2}}. \qquad (9)$$

To derive Eq. (7), we use the sum rule, $\sum_k \hbar g_k^2/\omega_k = E_C$, which can be shown for a general light-matter-type

Hamiltonian [56]. The new frame [Eq. (7)] gives a proper basis to extend Wilson's NRG approach to RSJ [51,57].

Benchmark results: The boundary sine-Gordon model.—Before analyzing the exact RSJ Hamiltonian [Eq. (7)], we start from benchmarking our NRG analysis for the boundary sine-Gordon (bsG) model [6,7,22,24,41,58]:

$$\hat{H}_{\mathrm{bsG}} = -E_J \cos\left[\frac{\hat{\phi}(0)}{\sqrt{\alpha}}\right] + \hat{H}_{\mathrm{TLL}}, \tag{10}$$

which can be obtained by taking the limit $\nu \to 0$ in Eq. (7). Its ground-state properties are well understood from the perturbative analysis, which predicts the transition at $\alpha = 1$. When $\alpha > 1$, the Josephson coupling E_J is relevant and, in the original frame [Eq. (1)], leads to the phase localization around $\varphi \sim 2\pi\mathbb{Z}$. In other words, the ground state is phase-coherent and superconducting. Conversely, when $\alpha < 1$, the Josephson energy E_J renormalizes to zero and the charge becomes localized, i.e., the system is insulating.

To numerically determine the transition point, we use the dc phase mobility, $\mu \equiv \alpha/(2\pi)\lim_{\omega\to+0}\omega\langle\varphi\varphi\rangle_\omega$, that becomes zero (nonzero) in the SC (insulator) phase, where $\langle\varphi\varphi\rangle_\omega$ is the Fourier transform of the ground-state phase correlation function [15,17,31]. In the transformed frame, we can express it as

$$\mu = \lim_{\omega\to+0}\sum_{n=0}^{\infty}\omega_{n0}\mu_{n0}\delta(\omega-\omega_{n0}), \tag{11}$$

$$\mu_{n0} \equiv \alpha|\langle 0|\hat{\Xi}|n\rangle|^2, \tag{12}$$

where ω_{n0} is the nth excitation frequency, and we introduce the mobility matrix element μ_{n0} with $|n\rangle$ being the nth energy eigenstate in the frame after the unitary transformation. We find that it suffices to calculate the dominant matrix element μ_{10} for the purpose of locating the transition point.

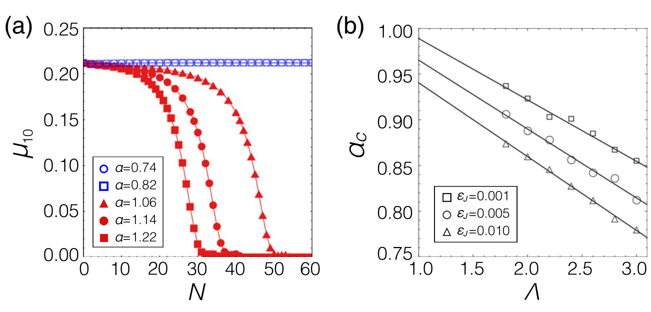

FIG. 2. NRG benchmark results in the bsG model [Eq. (10)]. (a) Flows of the mobility μ_{10} plotted against the number of RG steps N. In the SC phase $\alpha > \alpha_c$, the mobility flows to zero (red curves), while it remains nonzero in the insulator phase $\alpha < \alpha_c$ (blue curves). Parameters are $\epsilon_J = 0.001$ and $\Lambda = 2.0$. (b) Extrapolations of the critical value α_c to the Wilson parameter $\Lambda \to 1$. The scaling limit $\epsilon_J = E_J/\hbar W \to 0$ leads to the transition point $\alpha_c = 0.99(2)$, which agrees with the analytical value $\alpha_c = 1$.

Typical NRG flows of μ_{10} in the bsG model are shown in Fig. 2(a). As the energy scale is renormalized to lower regimes, the mobility eventually converges to zero in the SC phase $\alpha > \alpha_c$, while it remains nonzero in the insulator phase $\alpha < \alpha_c$. For each Wilson parameter Λ, we determine the critical value $\alpha_c(\Lambda)$ by estimating the crossover scale $N(\alpha)$ from NRG flows of μ_{10} and assuming $N(\alpha) \propto (\alpha-\alpha_c)^{-1}$. We then extrapolate the results to $\Lambda \to 1$ and locate the transition point [59]. As shown in Fig. 2(b), our NRG results are consistent with the analytical value $\alpha_c = 1$ in the scaling limit $\epsilon_J \equiv E_J/\hbar W \to 0$.

Previous studies used the bsG model [Eq. (10)] as a supposedly effective Hamiltonian of RSJ, which led to the vertical phase boundary at $\alpha_c = 1$ [red dashed line in Fig. 1(a)]. The rationale behind this argument is that the capacitance term ν is expected to be irrelevant from its scaling dimension and thus might be simply taken to be zero in Eq. (7) while replacing UV cutoff by $\alpha E_C/(\pi\hbar)$ without affecting low-energy physics [24,41]. However, the validity of this treatment must be carefully reexamined because the UV theory [Eq. (7)] possesses a large capacitance term $\nu \gg 1$, and its low-energy theory may go beyond perturbative regimes during RG processes before reaching to a fixed point with $\nu = 0$. To make concrete predictions, we thus need to resort to a nonperturbative analysis that consistently incorporates possible renormalization induced by the capacitance term ν.

NRG analysis of the exact RSJ Hamiltonian.—To achieve this, we now apply the NRG approach to the exact RSJ Hamiltonian [Eq. (7)]. To be concrete, we fix the charging energy $\epsilon_C = E_C/(\hbar W) = 0.05$ and vary the Josephson coupling as $0 < E_J/E_C \lesssim 0.4$, for which the dimensionless couplings satisfy the wideband condition

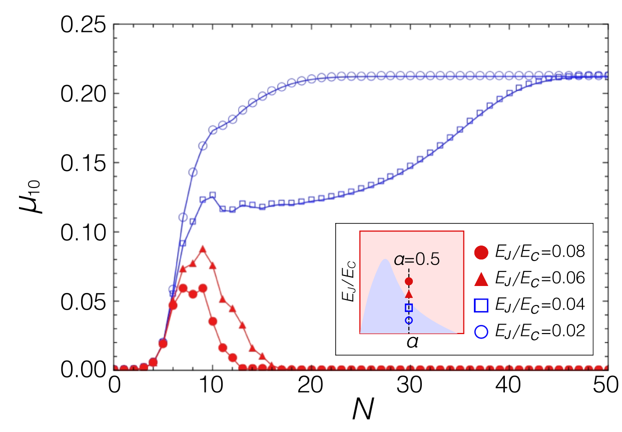

FIG. 3. NRG flows of μ_{10} in the exact RSJ Hamiltonian [Eq. (7)] at different E_J/E_C. The inset indicates the corresponding parameter regions in the phase diagram. The system flows to the insulator fixed point with nonzero μ_{10} when E_J/E_C is sufficiently small (blue curves). In contrast, the system nonmonotonically flows to the SC fixed point with zero μ_{10} if E_J/E_C surpasses a critical value (red curves). Parameters are $\alpha = 0.5$, $\Lambda = 2.0$, and $\epsilon_C = 0.05$.

$\epsilon_{J,C} \ll 1$ at UV scale. We confirm that our NRG analysis is already converged against the wideband limit [51]. Figure 3 shows typical NRG flows of μ_{10} at $\alpha = 0.5$. At the beginning of RG procedures, the mobility μ_{10} always grows and the system tends to flow into the insulator phase. When E_J/E_C is sufficiently small, μ_{10} keeps increasing and the system ultimately reaches to the insulator fixed point (blue curves in Fig. 3). Surprisingly, when E_J/E_C surpasses a certain threshold value $(E_J/E_C)_c$, the mobility μ_{10} turns from increasing to decreasing during RG processes and the system eventually flows to the SC fixed point (red curves in Fig. 3). The convergence of these flows becomes slower as one gets closer to the transition point (e.g., $E_J/E_C = 0.04$ in Fig. 3). We determine critical values $(E_J/E_C)_c$ shown in Fig. 1(a) by extrapolating the Wilson parameter $\Lambda \to 1$ for each α [51].

Figure 4 shows fixed-point values of the phase coherence $\langle \cos(\varphi) \rangle$ and the mobility μ_{10} at different α and E_J/E_C. The phase coherence gives inductive contribution to supercurrent carried by the ground state [38,60,61]. The behaviors of $\langle \cos(\varphi) \rangle$ and μ_{10} are consistent with each other; $\langle \cos(\varphi) \rangle$ vanishes and μ_{10} becomes nonzero in the insulator phase while the opposite is true in the superconducting phase. These results clearly indicate that the superconducting (insulating) phase at $\alpha > 0$ corresponds to the phase-localized (phase-delocalized) phase. It is also notable that both $\langle \cos(\varphi) \rangle$ and μ_{10} unambiguously indicate the reentrant transition from the insulator to SC phase as the resistance R

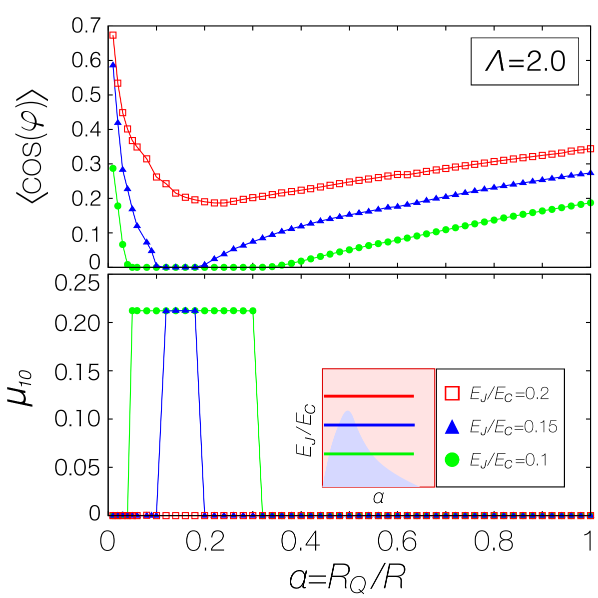

FIG. 4. Phase coherence $\langle \cos(\varphi) \rangle$ and the mobility μ_{10} plotted against $\alpha = R_Q/R$. The inset indicates the corresponding parameter regions in the phase diagram at $\Lambda = 2.0$. At sufficiently large E_J/E_C, the system always resides in the SC phase (red curve). When E_J/E_C is lower than a critical value $(E_J/E_C)_c$, there appears the insulating region as well as the reentrant transition into the SC phase in $\alpha \ll 1$ (green and blue curves). Parameters are $\Lambda = 2.0$ and $\epsilon_C = 0.02$.

is significantly increased beyond R_Q (i.e., $\alpha \ll 1$). In fact, in the limit $R \to \infty$, JJ completely decouples from the environment and should remain superconducting [cf. Eq. (1)]; our results in Figs. 4 and 1(a) are consistent with this expectation.

FRG analysis.—To understand these NRG results on a deeper level, we employ a nonperturbative analytical approach known as the FRG [62,63]. We use the functional ansatz retaining the most relevant Fourier mode, $\cos(\varphi)$, and go beyond the local potential approximation by including the (field-independent) wave function renormalization, resulting in the following set of flow equations [51]:

$$d_l \ln \epsilon_J = 1 - \int_0^\infty \frac{dy}{\pi} g(y), \tag{13}$$

$$d_l \ln \epsilon_C^{-1} = -1 + \epsilon_J^2 \int_0^\infty \frac{dy}{\pi} h(y), \tag{14}$$

where $l = \ln(\Lambda_0/\Lambda)$ is the logarithmic RG scale, the dimensionless parameters satisfy $\epsilon_{J(C)} = E_{J(C)}/\Lambda_0 \ll 1$ at UV scale $\Lambda = \Lambda_0$, and the integrals of g, h give positive values [51].

When $\epsilon_J \ll 1$, the flow equation [Eq. (13)] has the simple asymptotes depending on ϵ_C,

$$d_l \ln \epsilon_J \overset{\epsilon_J \ll 1}{\simeq} \begin{cases} 1 - \frac{\sqrt{2\epsilon_C}}{8} > 0 & \epsilon_C^{-1} \gg 1 \\ 1 - \frac{1}{\alpha} & \epsilon_C^{-1} \to 0 \end{cases}, \tag{15}$$

the latter of which reproduces the well-known perturbative result implying the *presence* of DQPT at $\alpha_c = 1$ [24]. Notably, however, the former shows that the Josephson coupling ϵ_J is relevant at any α in UV regimes. This fact together with Eq. (14) suggests that the supposedly irrelevant term $\nu \propto \epsilon_C^{-1}$ can significantly grow at low-energy scales due to the nonperturbative corrections, i.e., it can be dangerously irrelevant.

To determine fixed points the theory ultimately flows to, we numerically solve Eqs. (13) and (14), and obtain the flow diagram in Fig. 1(b) [64]. Because of the dangerously irrelevant term, when E_J/E_C is larger than a critical value, the theory flows into the SC fixed point even when $\alpha < 1$, leading to the *absence* of DQPT in transmon regimes. The insulator phase is then strongly suppressed to deep charge regimes $E_J/E_C \ll 1$ with $\alpha < 1$ [65].

At any E_J/E_C, the theory initially flows in favor of the insulator phase since the ratio obeys $d_l(\epsilon_J/\epsilon_C) < 0$ in UV regimes $\epsilon_{J,C} \ll 1$. At an intermediate low-energy scale, however, the theory enters nonperturbative regimes and can eventually exhibit the bifurcating flows to different fixed points depending on E_J/E_C [top panel in Fig. 1(b)]. This competition between renormalized Josephson and charging couplings explains the nonmonotonic NRG flows found in Fig. 3.

Discussions.—The proposed phase boundary in Fig. 1(a) is not vertical, which may appear to contradict with what is expected from the duality argument [15,16,22,24]. This apparent inconsistency originates from the dangerously irrelevant term ν discussed above. Indeed, only if ν can be safely neglected can one establish the duality between the weak and strong corrugation regimes [22,51].

In the strong corrugation regime $E_J/E_C \gg 1$, it was argued [15,22] that the RSJ Hamiltonian can be approximated by the tight-binding model of phase localized states at $\varphi = 2\pi\mathbb{Z}$. This model exhibits the transition at $\alpha_c = 1$, which seems to be inconsistent with our results showing the absence of transition in transmon regimes. This apparent contradiction originates from a failure of the tight-binding description under the wideband condition $E_C \ll \hbar W$, in which a cutoff-dependent term invalidates the level truncation in each cosine well [51].

Meanwhile, if one considers the opposite limit $E_C \gg \hbar W$, both the tight-binding description and the duality argument are expected to be valid without such ambiguities. This parameter regime corresponds to the left sides of our FRG phase diagram [Fig. 1(b)]. Indeed, in this limit, our results are consistent with the previous results predicting the transition at $\alpha_c = 1$ for any E_J/E_C.

To experimentally test our predictions, one has to take account of the lowest transmission-line frequency $\omega_{\min} = \pi v/L$ and finite temperature $k_B T$, which effectively introduce an IR cutoff in RG flows. One needs to renormalize to a sufficiently low-energy scale to attain small $\langle\cos(\varphi)\rangle$ close to a fixed-point value; this requires a sufficiently large system size and low temperature. For typical parameters of the insulator phase, $\alpha = 0.3$ and $E_J/E_C = 0.04$, one needs $\hbar\omega_{\min}, k_B T \lesssim 0.01 E_C$ to attain $\langle\cos\varphi\rangle \lesssim 10^{-2}$ [51]. These conditions are within reach of recent experiments [66–69] that have realized galvanic coupling of JJ to a high-impedance long transmission line. In particular, Refs. [66,67] realize $E_C/h = 5.4$ GHz, $\omega_{\min}/2\pi = 63$ MHz, $L \simeq 10$ mm, and UV cutoff $W/2\pi \simeq 20$ GHz in superconducting waveguides, while E_J is flux-tunable. These parameters correspond to $\hbar\omega_{\min}/E_C \simeq 0.01$ and $k_B T/E_C \simeq T/250$ mK. Thus, we expect that DQPT can be observed in this parameter region at millikelvin temperatures. We note that our estimation seems to be consistent with recent report of absence of DQPT [38], on which we speculate that the experimental parameters $E_C/h = 13$–54 GHz, $L = 16$ μm lead to finite-size effects causing residual phase coherence $\langle\cos(\varphi)\rangle$ [70].

In summary, we provided a comprehensive understanding of the dissipative quantum phase transition in a Josephson junction, which has been controversial for many years. We performed both numerical and analytical nonperturbative renormalization group analyses and obtained the phase diagram (Fig. 1) in which the insulator phase is strongly suppressed to the deep charge regime while, in the transmon regime, the system remains superconducting at any dissipation strengths. The origin of the failure of conventional understandings was traced to a previously overlooked dangerously irrelevant term that turns out to be relevant in genuinely nonperturbative regimes. Physically, this renormalization behavior corresponds to the eventual decrease of charging energy at low energies, which ultimately results in the enhancement of E_J/E_C and the phase localization. Our analysis and understanding developed here can be applied to a variety of systems ranging from strongly interacting light-matter systems to electron-phonon problems. We hope that our work stimulates further studies in these directions.

We are grateful to Eugene Demler, Shunsuke Furukawa, Atac Imamoglu, Hosho Katsura, Naoto Nagaosa, Masahito Ueda, and Takeru Yokota for fruitful discussions. Y. A. acknowledges support from the Japan Society for the Promotion of Science through Grants No. JP19K23424 and No. JP21K13859. M. O. is supported in part by MEXT/JSPS KAKENHI Grants No. JP17H06462 and No. JP19H01808, JST CREST Grant No. JPMJCR19T2.

*Corresponding author.
masuki@g.ecc.u-tokyo.ac.jp
†Corresponding author.
ashida@phys.s.u-tokyo.ac.jp

[1] J. Kondo, Prog. Theor. Phys. **32**, 37 (1964).
[2] P. W. Anderson, Phys. Rev. **124**, 41 (1961).
[3] I. Affleck, A. W. W. Ludwig, H.-B. Pang, and D. L. Cox, Phys. Rev. B **45**, 7918 (1992).
[4] M. Pustilnik and L. Glazman, J. Phys. Condens. Matter **16**, R513 (2004).
[5] H. v. Löhneysen, A. Rosch, M. Vojta, and P. Wölfle, Rev. Mod. Phys. **79**, 1015 (2007).
[6] C. L. Kane and M. P. A. Fisher, Phys. Rev. B **46**, 15233 (1992).
[7] A. Furusaki and N. Nagaosa, Phys. Rev. B **47**, 4631 (1993).
[8] M. Oshikawa, C. Chamon, and I. Affleck, J. Stat. Mech. 02 (2006) P02008.
[9] M. Bockrath, D. H. Cobden, J. Lu, A. G. Rinzler, R. E. Smalley, L. Balents, and P. L. McEuen, Nature (London) **397**, 598 (1999).
[10] Z. Yao, H. W. C. Postma, L. Balents, and C. Dekker, Nature (London) **402**, 273 (1999).
[11] A. O. Caldeira and A. J. Leggett, Phys. Rev. Lett. **46**, 211 (1981); Ann. Phys. (N.Y.) **149**, 374 (1983); Physica (Amsterdam) **121A**, 587 (1983).
[12] A. J. Leggett, S. Chakravarty, A. T. Dorsey, M. P. A. Fisher, A. Garg, and W. Zwerger, Rev. Mod. Phys. **59**, 1 (1987).
[13] F. B. Anders, R. Bulla, and M. Vojta, Phys. Rev. Lett. **98**, 210402 (2007).
[14] K. L. Hur, Ann. Phys. (Amsterdam) **323**, 2208 (2008).
[15] A. Schmid, Phys. Rev. Lett. **51**, 1506 (1983).
[16] S. Bulgadaev, JETP Lett. **39**, 264 (1984), http://jetpletters.ru/ps/1289/article_19477.shtml.
[17] G. Schön and A. Zaikin, Phys. Rep. **198**, 237 (1990).
[18] N. Nagaosa, *Quantum Field Theory in Condensed Matter Physics* (Springer Science & Business Media, New York, 1999).

[19] B. I. Halperin, G. Refael, and E. Demler, Int. J. Mod. Phys. B **24**, 4039 (2010).
[20] U. Weiss, *Quantum Dissipative Systems*, 3rd ed. (World Scientific, Singapore, 2008).
[21] A. Kapitulnik, S. A. Kivelson, and B. Spivak, Rev. Mod. Phys. **91**, 011002 (2019).
[22] F. Guinea, V. Hakim, and A. Muramatsu, Phys. Rev. Lett. **54**, 263 (1985).
[23] C. Aslangul, N. Pottier, and D. Saint-James, Phys. Lett. A **111**, 175 (1985).
[24] M. P. A. Fisher and W. Zwerger, Phys. Rev. B **32**, 6190 (1985).
[25] A. Zaikin and S. Panyukov, Phys. Lett. A **120**, 306 (1987).
[26] U. Weiss and H. Grabert, Phys. Lett. A **108**, 63 (1985).
[27] D. Averin, Y. Nazarov, and A. Odintsov, Physica (Amsterdam) **165–166B**, 945 (1990).
[28] C. Callan and L. Thorlacius, Nucl. Phys. **B329**, 117 (1990).
[29] G. Refael, E. Demler, Y. Oreg, and D. S. Fisher, Phys. Rev. B **68**, 214515 (2003); **75**, 014522 (2007).
[30] C. P. Herrero and A. D. Zaikin, Phys. Rev. B **65**, 104516 (2002).
[31] N. Kimura and T. Kato, Phys. Rev. B **69**, 012504 (2004).
[32] P. Werner and M. Troyer, Phys. Rev. Lett. **95**, 060201 (2005); Prog. Theor. Phys. Suppl. **160**, 395 (2005); S. L. Lukyanov and P. Werner, J. Stat. Mech. (2007) P06002.
[33] L. S. Kuzmin, Y. V. Nazarov, D. B. Haviland, P. Delsing, and T. Claeson, Phys. Rev. Lett. **67**, 1161 (1991).
[34] R. Yagi, S. Kobayashi, and Y. Ootuka, J. Phys. Soc. Jpn. **66**, 3722 (1997).
[35] J. S. Penttilä, U. Parts, P. J. Hakonen, M. A. Paalanen, and E. B. Sonin, Phys. Rev. Lett. **82**, 1004 (1999).
[36] J. S. Penttilä, P. Hakonen, E. Sonin, and M. Paalanen, J. Low Temp. Phys. **125**, 89 (2001).
[37] G. Liu, Y. Zhang, and C. N. Lau, Phys. Rev. Lett. **102**, 016803 (2009).
[38] A. Murani, N. Bourlet, H. le Sueur, F. Portier, C. Altimiras, D. Esteve, H. Grabert, J. Stockburger, J. Ankerhold, and P. Joyez, Phys. Rev. X **10**, 021003 (2020).
[39] P. J. Hakonen and E. B. Sonin, Phys. Rev. X **11**, 018001 (2021).
[40] A. Murani, N. Bourlet, H. le Sueur, F. Portier, C. Altimiras, D. Esteve, H. Grabert, J. Stockburger, J. Ankerhold, and P. Joyez, Phys. Rev. X **11**, 018002 (2021).
[41] I. Affleck, M. Oshikawa, and H. Saleur, Nucl. Phys. **B594**, 535 (2001).
[42] Y. Nakamura, Y. A. Pashkin, and J. Tsai, Nature (London) **398**, 786 (1999).
[43] A. Blais, A. L. Grimsmo, S. M. Girvin, and A. Wallraff, Rev. Mod. Phys. **93**, 025005 (2021).
[44] M. Goldstein, M. H. Devoret, M. Houzet, and L. I. Glazman, Phys. Rev. Lett. **110**, 017002 (2013).
[45] J. Leppäkangas, J. Braumüller, M. Hauck, J.-M. Reiner, I. Schwenk, S. Zanker, L. Fritz, A. V. Ustinov, M. Weides, and M. Marthaler, Phys. Rev. A **97**, 052321 (2018).
[46] K. Kaur, T. Sépulcre, N. Roch, I. Snyman, S. Florens, and S. Bera, Phys. Rev. Lett. **127**, 237702 (2021).
[47] I. V. Pechenezhskiy, R. A. Mencia, L. B. Nguyen, Y.-H. Lin, and V. E. Manucharyan, Nature (London) **585**, 368 (2020).
[48] M. Houzet and L. I. Glazman, Phys. Rev. Lett. **125**, 267701 (2020).
[49] A. Burshtein, R. Kuzmin, V. E. Manucharyan, and M. Goldstein, Phys. Rev. Lett. **126**, 137701 (2021).
[50] C. Cohen-Tannoudji, J. Dupont-Roc, and G. Grynberg, *Photons and Atoms* (Wiley, New York, 1989).
[51] See Supplemental Materials at http://link.aps.org/supplemental/10.1103/PhysRevLett.129.087001 for further details on the statements and the derivations.
[52] M. F. Gely, A. Parra-Rodriguez, D. Bothner, Y. M. Blanter, S. J. Bosman, E. Solano, and G. A. Steele, Phys. Rev. B **95**, 245115 (2017).
[53] M. Malekakhlagh, A. Petrescu, and H. E. Türeci, Phys. Rev. Lett. **119**, 073601 (2017).
[54] A. Parra-Rodriguez, E. Rico, E. Solano, and I. L. Egusquiza, Quantum Sci. Technol. **3**, 024012 (2018).
[55] K. G. Wilson, Rev. Mod. Phys. **47**, 773 (1975).
[56] Y. Ashida, A. Imamoglu, and E. Demler, Phys. Rev. Lett. **126**, 153603 (2021); , Phys. Rev. Research **4**, 023194 (2022).
[57] Because the "kinetic energy" term $E_C\hat{N}^2$ disappears via the unitary transformation, eigenstates of $\hat{N}$ are not an appropriate basis to analyze the low-energy physics; this causes a failure of NRG or two-state approximation in the frame of Eq. (3).
[58] P. Fendley, A. W. W. Ludwig, and H. Saleur, Phys. Rev. Lett. **74**, 3005 (1995).
[59] R. Bulla, N.-H. Tong, and M. Vojta, Phys. Rev. Lett. **91**, 170601 (2003); R. Bulla, H.-J. Lee, N.-H. Tong, and M. Vojta, Phys. Rev. B **71**, 045122 (2005).
[60] P. Joyez, Phys. Rev. Lett. **110**, 217003 (2013).
[61] I. Safi and P. Joyez, Phys. Rev. B **84**, 205129 (2011).
[62] C. Wetterich, Phys. Lett. B **301**, 90 (1993).
[63] N. Dupuis, L. Canet, A. Eichhorn, W. Metzner, J. Pawlowski, M. Tissier, and N. Wschebor, Phys. Rep. **910**, 1 (2021).
[64] We remark that an apparent upper bound on the Josephson coupling at $\epsilon_J = 1$ in the flow diagram in Fig. 1(b) is an artifact due to our approximation that truncates (less relevant) higher-order Fourier modes $\cos(n\varphi)$ with $n \geq 2$.
[65] We confirm that the inclusion of higher Fourier modes does not affect our conclusions.
[66] R. Kuzmin, N. Mehta, N. Grabon, R. Mencia, and V. E. Manucharyan, npj Quantum Inf. **5**, 1 (2019).
[67] R. Kuzmin, N. Grabon, N. Mehta, A. Burshtein, M. Goldstein, M. Houzet, L. I. Glazman, and V. E. Manucharyan, Phys. Rev. Lett. **126**, 197701 (2021).
[68] J. P. Martínez, S. Léger, N. Gheeraert, R. Dassonneville, L. Planat, F. Foroughi, Y. Krupko, O. Buisson, C. Naud, W. Hasch-Guichard, S. Florens, I. Snyman, and N. Roch, npj Quantum Inf. **5**, 1 (2019).
[69] S. Léger, J. Puertas-Martínez, K. Bharadwaj, R. Dassonneville, J. Delaforce, F. Foroughi, V. Milchakov, L. Planat, O. Buisson, C. Naud, W. Hasch-Guichard, S. Florens, I. Snyman, and N. Roch, Nat. Commun. **10**, 5259 (2019).
[70] The resistor used in the experiment in Ref. [38] is a chromic resistor, and one may make a modest estimate of its IR cutoff $\sim v/L$ using the typical sound velocity of Chromium $v \sim 6 \times 10^3$ m/s.